SAND2011-6983C

Verification and Validation of SIERRA/Fuego in an Unconfined Upward Burning Solid Propellant Fire

October 17th, 2011

Allen Ricks
Fire and Aerosol Sciences
Sandia National Laboratories

Sandia is a multiprogram laboratory operated by Sandia Corporation, a Lockheed-Martin company, for the United States Department of Energy's National Nuclear Security Administration under contract DE-AC04-94AL85000

NNSA National Nuclear Security Administration

Sandia National Laboratories

Basic Background / Description of Propellant Fires

- Many solid rocket propellants contain aluminum particles (~17% - 19% of propellant by weight) that burn to provide additional thrust
- In an accident scenario the propellant typically burns at atmospheric pressure or a “low” pressure above ambient but well below the design pressure
- At these pressures the aluminum burns inefficiently and particles lofted off the surface of the propellant may burn over scales of meters
- Other components of the solid propellant burn in a thin layer near the propellant surface, rapidly expanding to produce a jet of hot products with a velocity of ~15 m/s

Cylindrical rod calorimeter suspended above an upward facing burning propellant charge. Photograph from Figueroa et al (2007).

Other Complicating Factors in Propellant Fires

- The aluminum particles in the solid rocket propellant melt inside and at the top surface of the propellant as the binder and oxidizer burn, and many particles may coalesce into a large droplet before being lofted off the surface
- Aluminum particles / droplets have an aluminum oxide cap or shell, and a range of behavior has been reported
- Aluminum combustion is energetic enough to produce very high temperatures (~3500K) in diffusion flames around droplets
- When aluminum burns it forms alumina (Al_2O_3), which condenses out as a fine solid particulate "smoke" that becomes a major player in radiative heat transfer

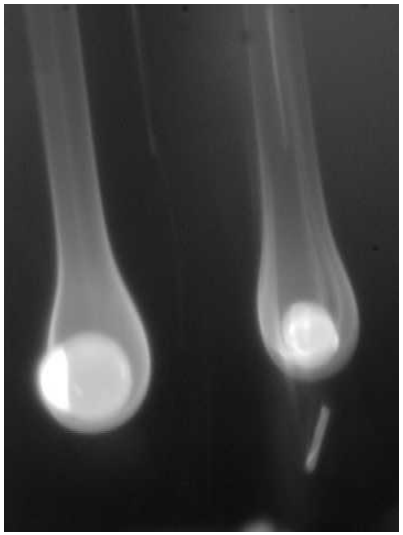

Burning aluminum droplets. Photograph from Parr and Hanson-Parr (2006).

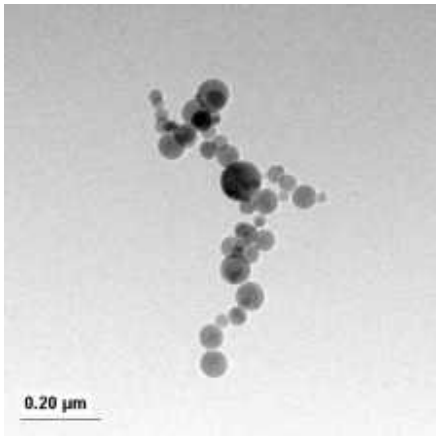

Alumina "smoke" particle (sizes of particles vary).

Key Features of Modeling Approach

- SIERRA/Fuego is a low Mach number fluid mechanics code with models to account for chemical reactions and radiative and convective heat transfer
- Fuego has been used extensively to simulate hydrocarbon fires
- Additional features in Fuego that are used in propellant fire simulations include:
  - A Lagrangian particle model with evaporation
  - An aluminum combustion model in O_2, CO_2, and/or H_2O
  - A model for the radiative properties of aluminum droplets, alumina smoke particles, and key gas phase species

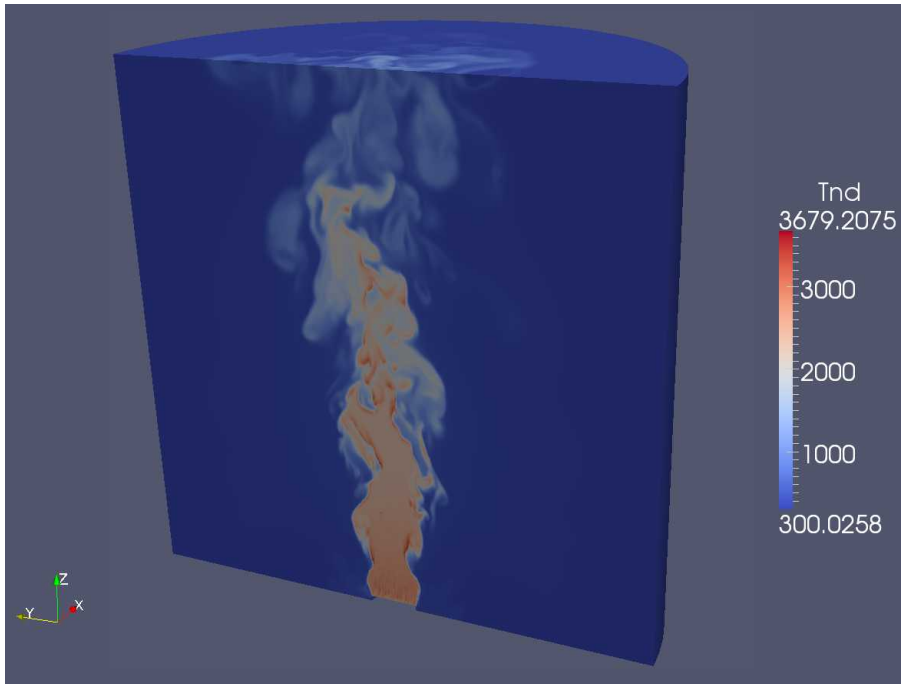

Products of propellant reaction (assuming no aluminum reactions) are introduced as an inflow boundary condition

Aluminum droplets are introduced near the inflow boundary and tracked as parcels of particles

Aluminum droplets evaporate and react to form alumina smoke

Gas phase species react with oxygen at edges of plume

Single Droplet Studies

- The basic fluid mechanics, gas phase reactions, and convection/radiation heat transfer in Fuego were already supported by a body of evidence
- The behavior of single aluminum droplets in Fuego simulations was studied prior to any attempt to validate simulations of an entire propellant fire
  - particle motion in fluid field
  - particle/fluid interactions in momentum, species, enthalpy, etc.
- The evaporation rates of single aluminum droplets in a variety of gas phase mixtures were compared to experimental data with mixed results

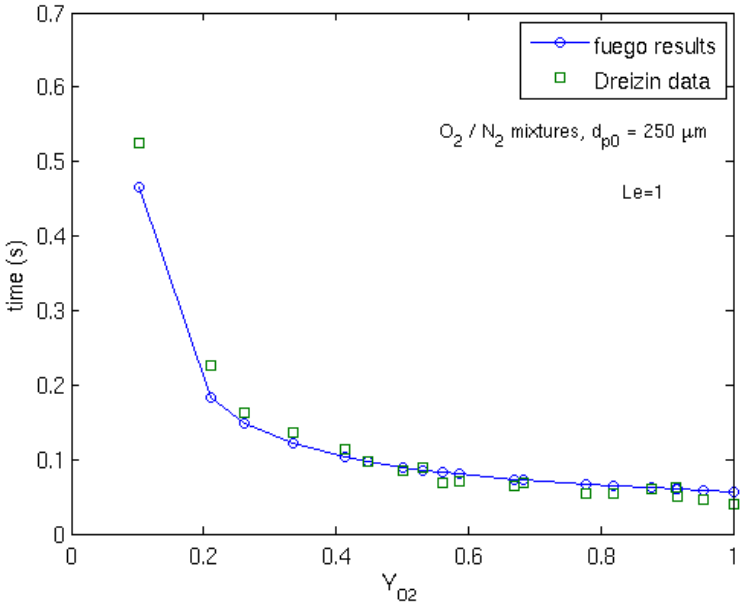

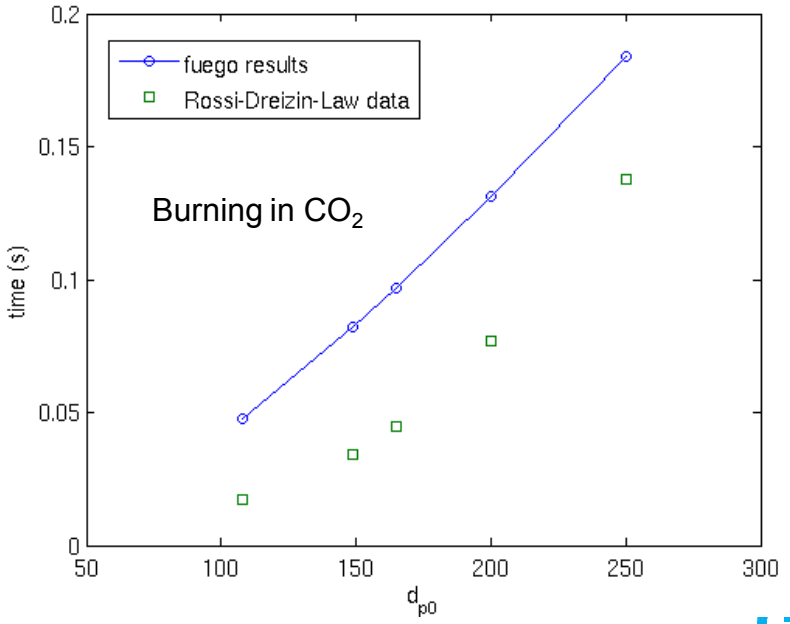

Propellant Fire Validation Test Cases

- A series of experiments have been performed to better understand propellant fire behavior and to obtain data for the validation of models
- Data sets selected for validation test cases include unobstructed upward burn tests (6”, 12”, and 18” charge diameters)
- Other data sets are available but have not yet been studied
- The propellant studied is an aluminized Al/AP/HTPB solid rocket propellant

#5 Welding Filter

No Filter

Upward Burn Experiments

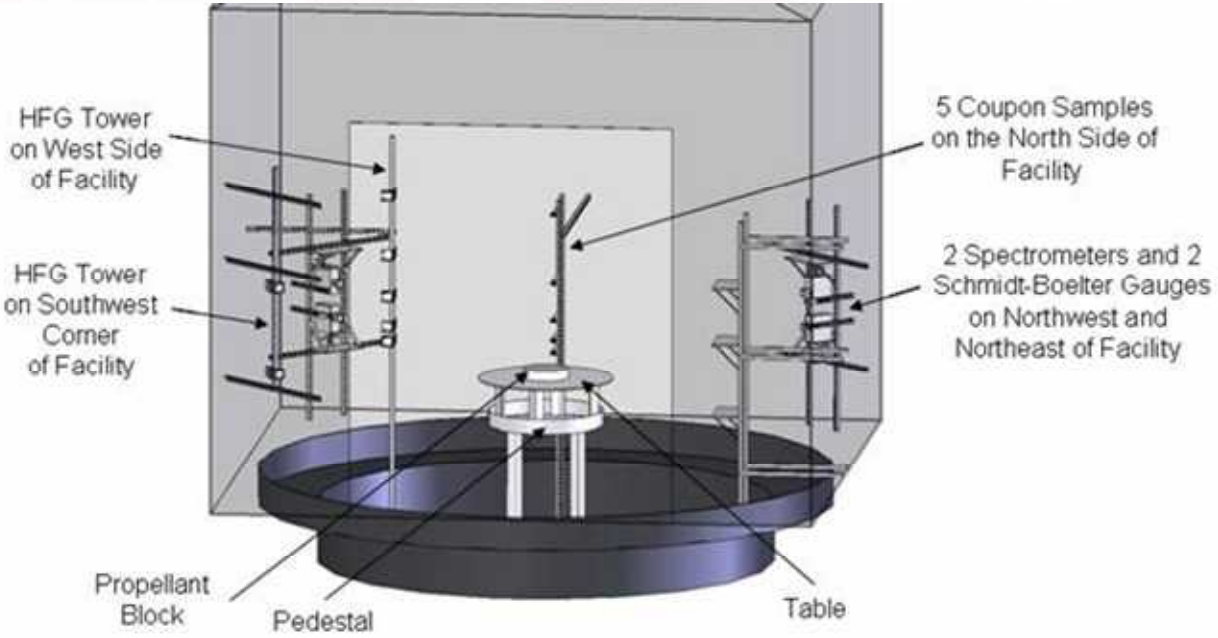

Upward-facing propellant charge pre-test

Upward-facing propellant charge post-test

Upward Burn Case Validation Approach

- The best experimental data available for comparison with model results are heat fluxes at a distance from the plume (5' from plume centerline, gages at 5 heights)
- A set of parameters was selected for a sensitivity study to determine which uncertain parameters contributed the greatest amount to the uncertainty in the predicted flux
    - Solution verification was also performed
- From the sensitivity study a set of parameter values were selected to provide a high heat flux case and a low heat flux case
- The simulation results were compared to the measurements plus uncertainty

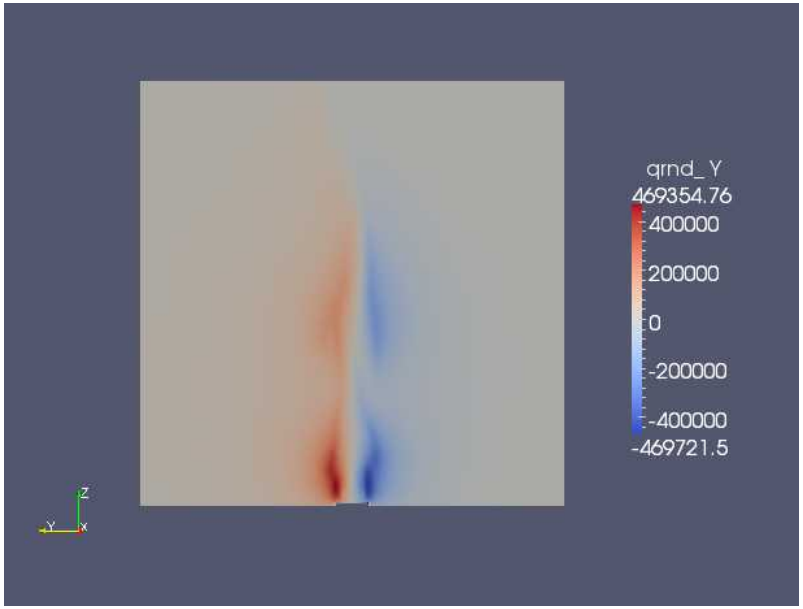

Upward Burn Solution Verification

- Simulations were performed to determine the sensitivity of the metric of interest to details of the solution (while still nominally solving the same equations)
- Parameters for solution verification included
  - Grid resolution
  - Time step
  - Aluminum droplet parcel size
  - Radiation quadrature order
  - Number of Picard loops
  - Upwinding factor

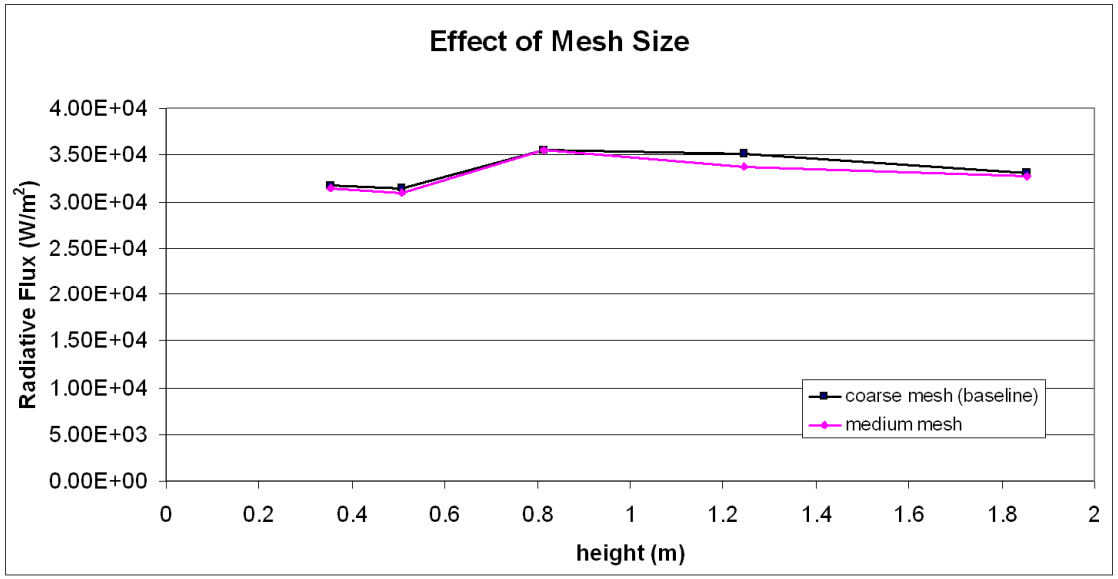

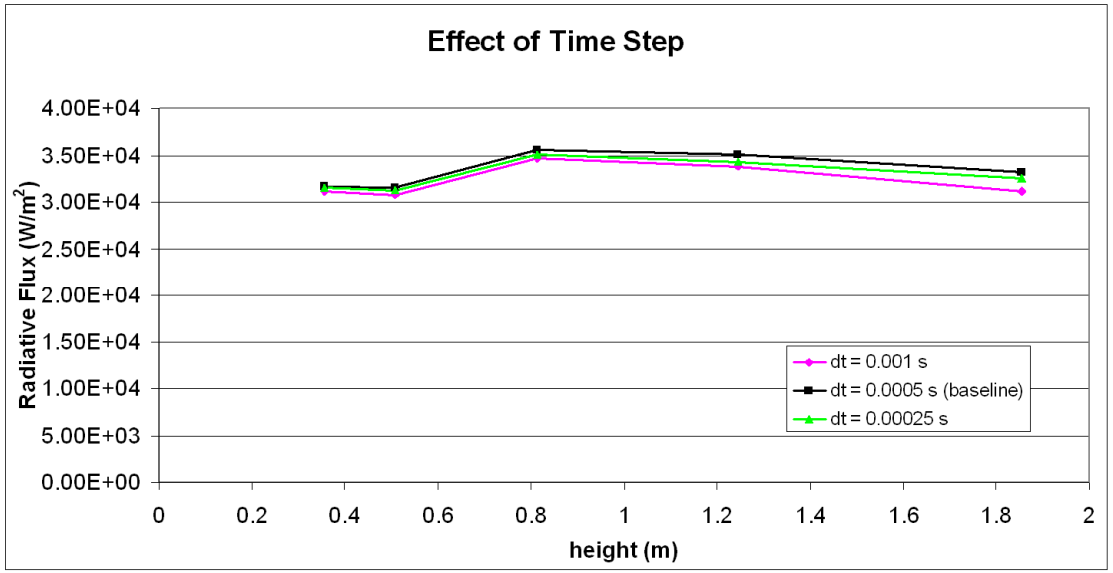

Upward Burn Solution Verification

- Simulations were performed to determine the sensitivity of the metric of interest to details of the solution (while still nominally solving the same equations)
- Parameters for solution verification included
  - Grid resolution
  - Time step
  - Aluminum droplet parcel size
  - Radiation quadrature order
  - Number of Picard loops
  - Upwinding factor

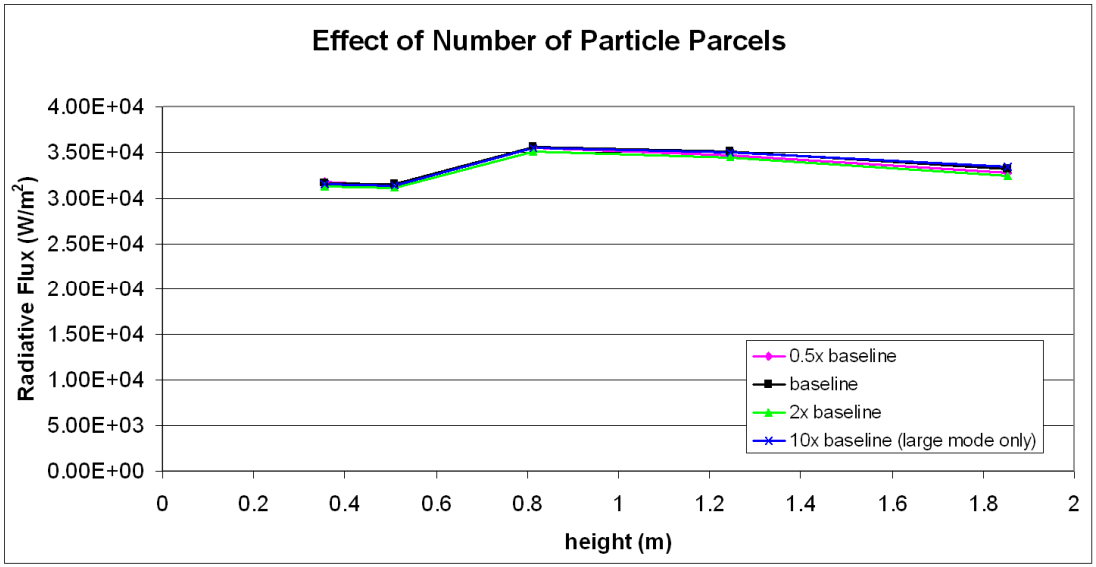

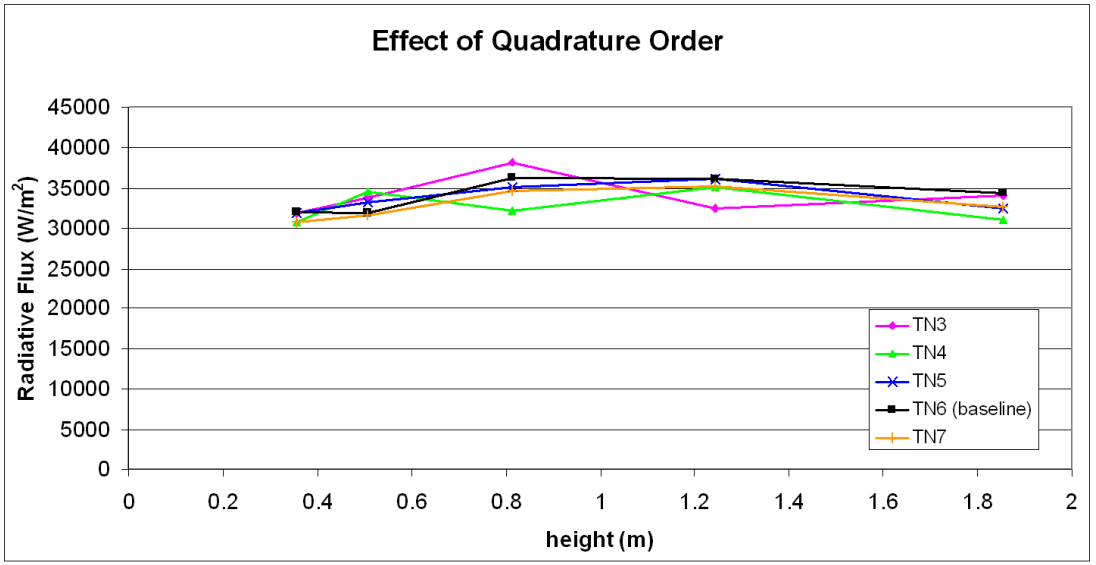

NNSA National Nuclear Security Administration

Sandia National Laboratories

Upward Burn Solution Verification

- Simulations were performed to determine the sensitivity of the metric of interest to details of the solution (while still nominally solving the same equations)
- Parameters for solution verification included
  - Grid resolution
  - Time step
  - Aluminum droplet parcel size
  - Radiation quadrature order
  - Number of Picard loops
  - Upwinding factor

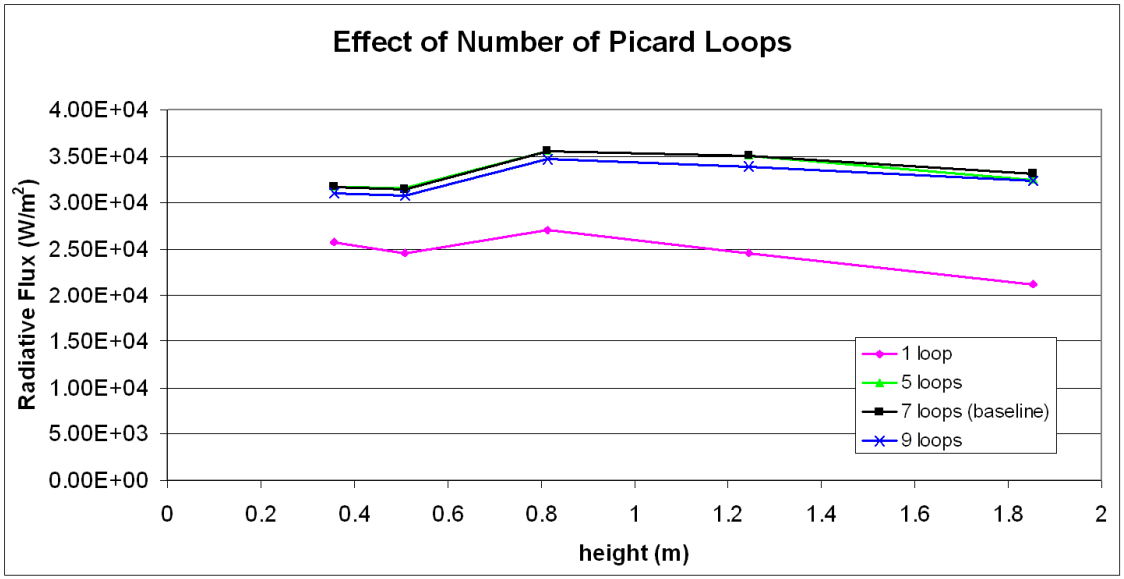

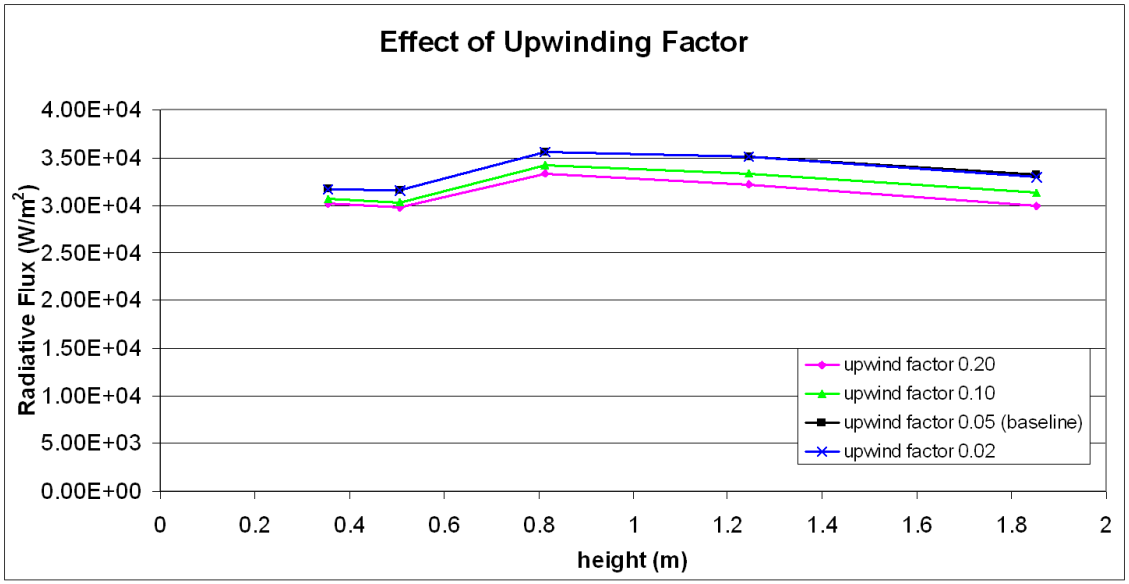

Upward Burn Sensitivity Study Parameters

Boundary Condition	Best Estimate	Range Estimate	Notes
mass burning rate		Depends on propellant test	the gas velocity and temperature at the boundary are determined from these two parameters
aluminum particle injection temperature	1800 K	1300 – 2300 K	
solid propellant surface temperature and emissivity		600 K and 0.9 to 1700 K and 0.2	
Al particle size distribution	Aerojet distribution	Thiokol distribution	2 discrete choices
Intrinsic Parameter	**Best Estimate**	**Range Estimate**	**Notes**
Prandtl numbers		0.3 - 0.7	affect diffusion of gas-phase aluminum away from particle
Schmidt numbers		0.6 - 0.7	
Diffusion Flame Temp		3200 - 3800 K	
aluminum emissivity	0.1	0.05 – 0.3	
alumina smoke absorption kernel	Brewster's model	Konopka Rocket 1 to Konopka Rocket 2	3 discrete choices
Model Form	**Primary Form**	**Other Form(s)**	
turbulence	TFNS	RANS	
combustion	raw	mixture fraction	← **These models (grayed boxes) were not ready in time to include in UQ study.**
scattering	Off	On	
alumina cap	Off	On	

Upward Burn Sensitivity Study Parameters

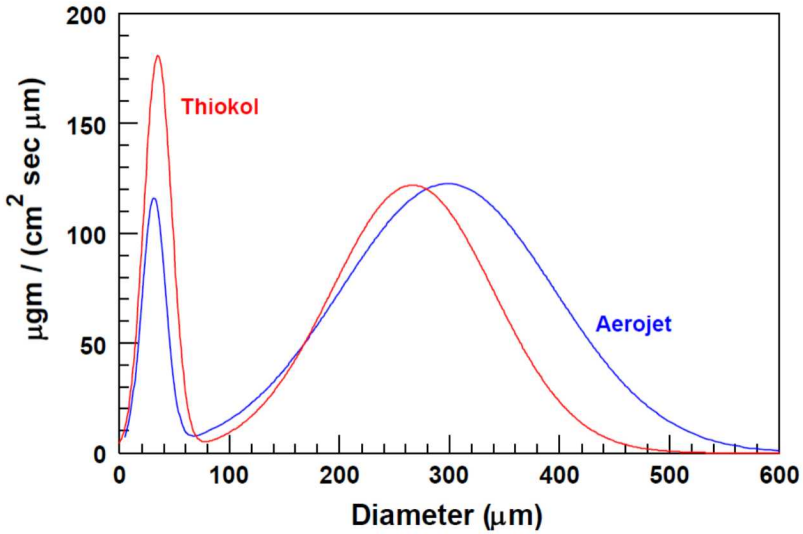

Difference between Aerojet and Thiokol particle size distributions (Parr and Hanson-Parr, 2006).

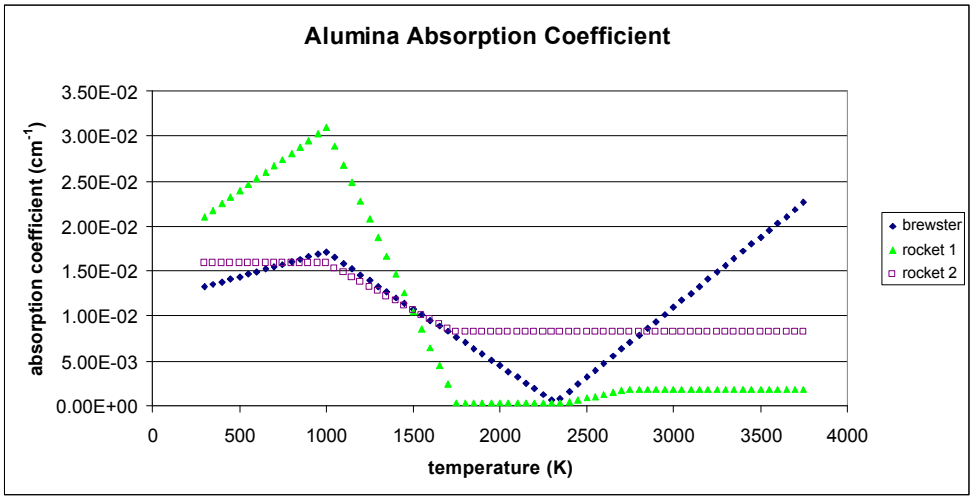

Alumina absorption coefficient models assuming $Y_{alumina}$ = 0.2 and $\rho_{mixture}$ = 0.2 kg/m^3.

Burn rates for upward burn tests.

Matrix #	Diameter (in.)	Time (s)			Linear rate (mm/s)			Mass rate (kg/m2-s)		
		Max.	Min.	Nom.	Max.	Min.	Nom.	Max.	Min.	Nom.
1R	18	120	106	113.0	0.847	0.958	0.899	1.519	1.719	1.613
2	12	126	105	115.5	0.806	0.968	0.880	1.446	1.736	1.578
3	6	116	108	112.0	0.876	0.941	0.907	1.571	1.687	1.627

Upward Burn Sensitivity Study Cases

Sim. #	Mass Burn Rate	Propellant Burn Surface Temp. & Emissivity	Al. Particle Injection Temp.	Al. Emissivity	Al. Particle Size Distribution	Diffusion Flame Temp.	Prandtl #	Schmidt #
	depends on test	600K, 0.9 to 1700K, 0.2	1300 – 2300K	Nom. = 0.1 range = 0.05 – 0.30	Nom. = Aerojet Alt. = Thiokol	3200K - 3800K	0.3 - 0.7	0.6 - 0.7
1	Mid	Mid	Mid	Nominal	Nominal	Mid	Mid	Mid
2	High	High	High	Nominal	Nominal	Mid	Mid	Mid
3	High	High	Low	Nominal	Nominal	Mid	Mid	Mid
4	High	Low	High	Nominal	Nominal	Mid	Mid	Mid
5	High	Low	Low	Nominal	Nominal	Mid	Mid	Mid
6	Low	High	High	Nominal	Nominal	Mid	Mid	Mid
7	Low	High	Low	Nominal	Nominal	Mid	Mid	Mid
8	Low	Low	High	Nominal	Nominal	Mid	Mid	Mid
9	Low	Low	Low	Nominal	Nominal	Mid	Mid	Mid
10	Mid	Mid	Mid	Low	Nominal	Mid	Mid	Mid
11	Mid	Mid	Mid	High	Nominal	Mid	Mid	Mid
12	Mid	Mid	Mid	Nominal	Alternate	Mid	Mid	Mid
13	Mid	Mid	Mid	Nominal	Nominal	Low	Mid	Mid
14	Mid	Mid	Mid	Nominal	Nominal	High	Mid	Mid
15	Mid	Mid	Mid	Nominal	Nominal	Mid	Low	Mid
16	Mid	Mid	Mid	Nominal	Nominal	Mid	High	Mid
17	Mid	Mid	Mid	Nominal	Nominal	Mid	Mid	Low
18	Mid	Mid	Mid	Nominal	Nominal	Mid	Mid	High
19	Same as case 1 except turbulence model form changes to from TFNS to RANS							
20	Same as case 1 except alumina absorption smoke kernel changes from Brewster to Rocket 1							
21	Same as case 1 except alumina absorption smoke kernel changes from Brewster to Rocket 2							

Upward Burn Sensitivity Study Results

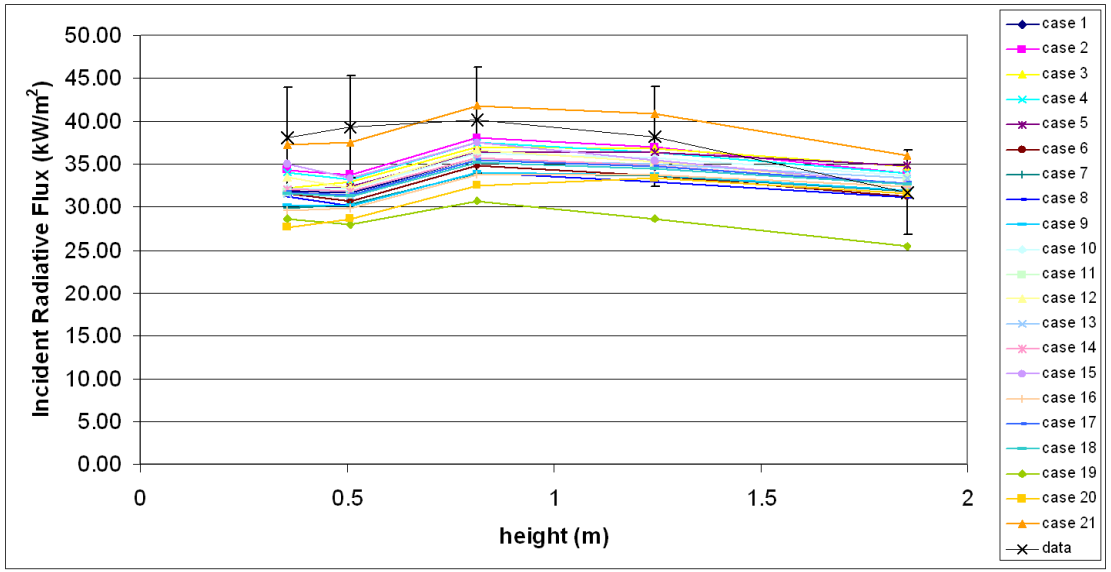

By comparing the response for each case the effects of the various parameter settings can be estimated

The parameter sensitivity information can then be used to select one or more high-flux cases and one or more low-flux cases

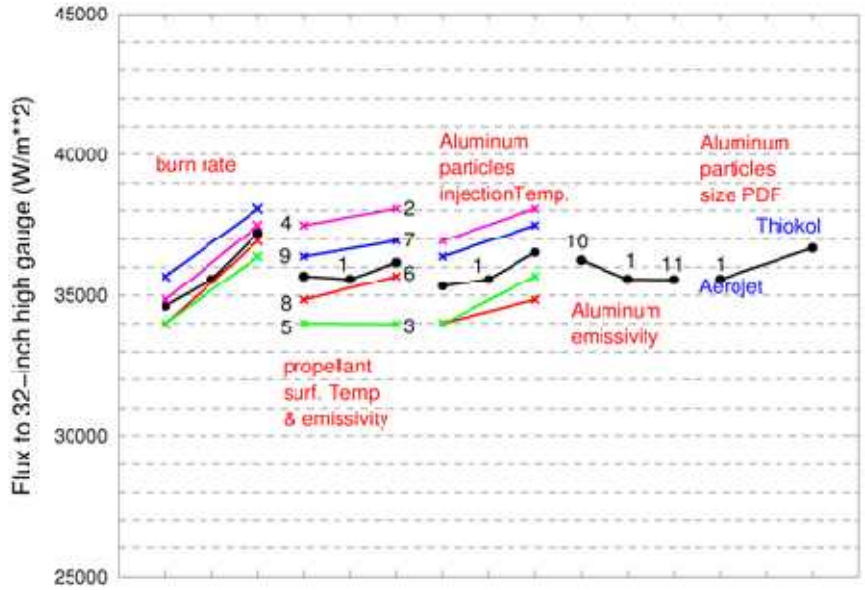

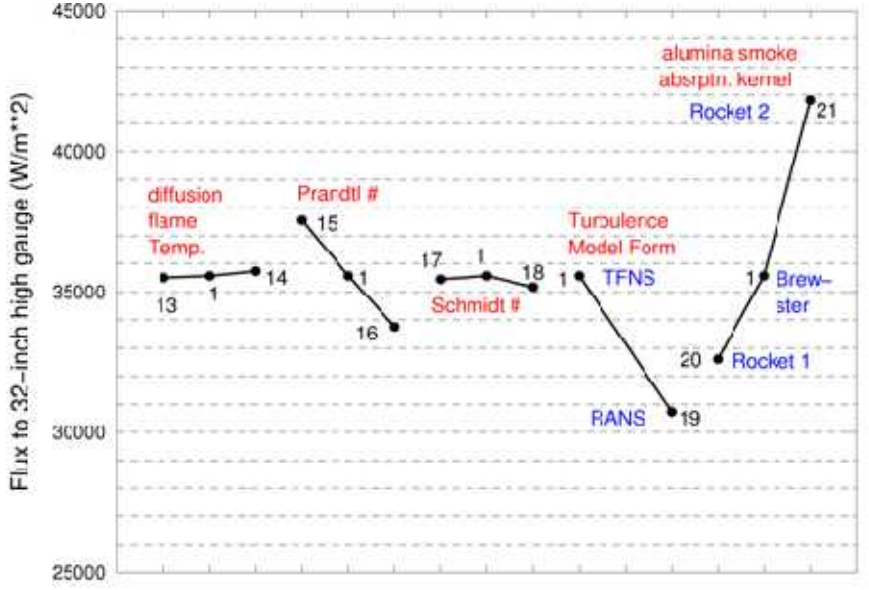

Upward Burn UQ Study Results

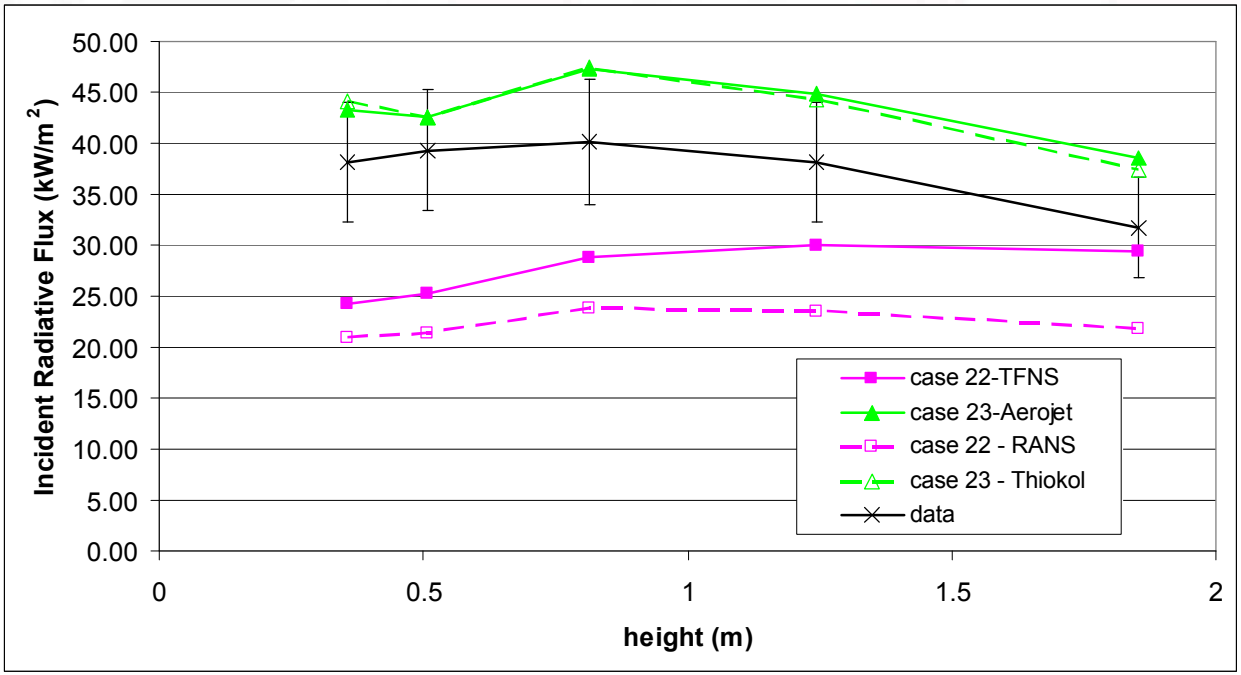

The uncertainty in model parameters and boundary conditions does not quite bound the experimental data (with uncertainty) at all heights, but the general level of agreement is encouraging

Sim. #	Mass Burn Rate	Propellant Burn Surface Temp. & Emissivity	Al. Particle Injection Temp.	Al. Emissivity	Al. Particle Size Distribution	Diffusion Flame Temp.	Prandtl #	Schmidt #
	Depends on test	**600K, 0.9 to 1700K, 0.2**	**1300 – 2300K**	**Nom. = 0.1 range = 0.05 – 0.30**	**Nominal = Aerojet, Alternate = Thiokol**	**3200K - 3800K**	**0.3 - 0.7**	**0.6 - 0.7**
22-lower	Low	Med	Low	High	Aerojet	Low	High	High
23-upper	High	High	High	Low	Thiokol	High	Low	Med
22 cont'd	turbulence model form = RANS | alumina absorption smoke kernel = Rocket 1							
23 cont'd	turbulence model form = TFNS | alumina absorption smoke kernel = Rocket 2							

Conclusions

- A propellant fire simulation capability exists in SIERRA/Fuego
- Agreement of predictions to experimental data is encouraging, but complete validation was not achieved
- Validation in other scenarios is highly desirable
- Additional physics models may help to resolve the differences and improve predictions
    - multi-component droplets
    - droplet stick / rebound / shatter model*
    - geometry effects of deposit layer*
    - geometry changes with propellant charge recession
    - scattering in radiation solve
    - “comet” emission model?

* for validation cases with impinging jets

References

Figueroa, V., Gill, W., and Erikson, W., “JPL-NASA Propellant Fire Test Series: Test Overview and Data Collected,” Sandia National Laboratories report to JPL, September 2007.

Hewson, J., Glaze, D., and Wagner, G. “A Lagrangian Model for Evolving Particulate Flows, Sprays and Combustion and Its Coupling to an Eulerian Fluid Solver,” draft Sandia National Laboratories report SAND2007-????, 2007.

Parr, T., and Hanson-Parr, D., “Near Field Combustion Characteristics of Aerojet Atlas Propellant,” Jacobs Sverdrup Naval Systems Group (under contract to Naval Air Warfare Center, Weapons Division, China Lake) progress report to JPL, 21 November 2006.

Parr, T., and Hanson-Parr, D., “AP/HTPB/Al Propellant Flame Structure at 1 atm,” Powerpoint presentation, Jacobs Sverdrup Naval Systems Group (under contract to Naval Air Warfare Center, Weapons Division, China Lake), 2006.

Backup / Additional Slides

- Aluminum droplet formation description and videos
- Aluminum combustion model formulation

Aluminum Droplet Formation

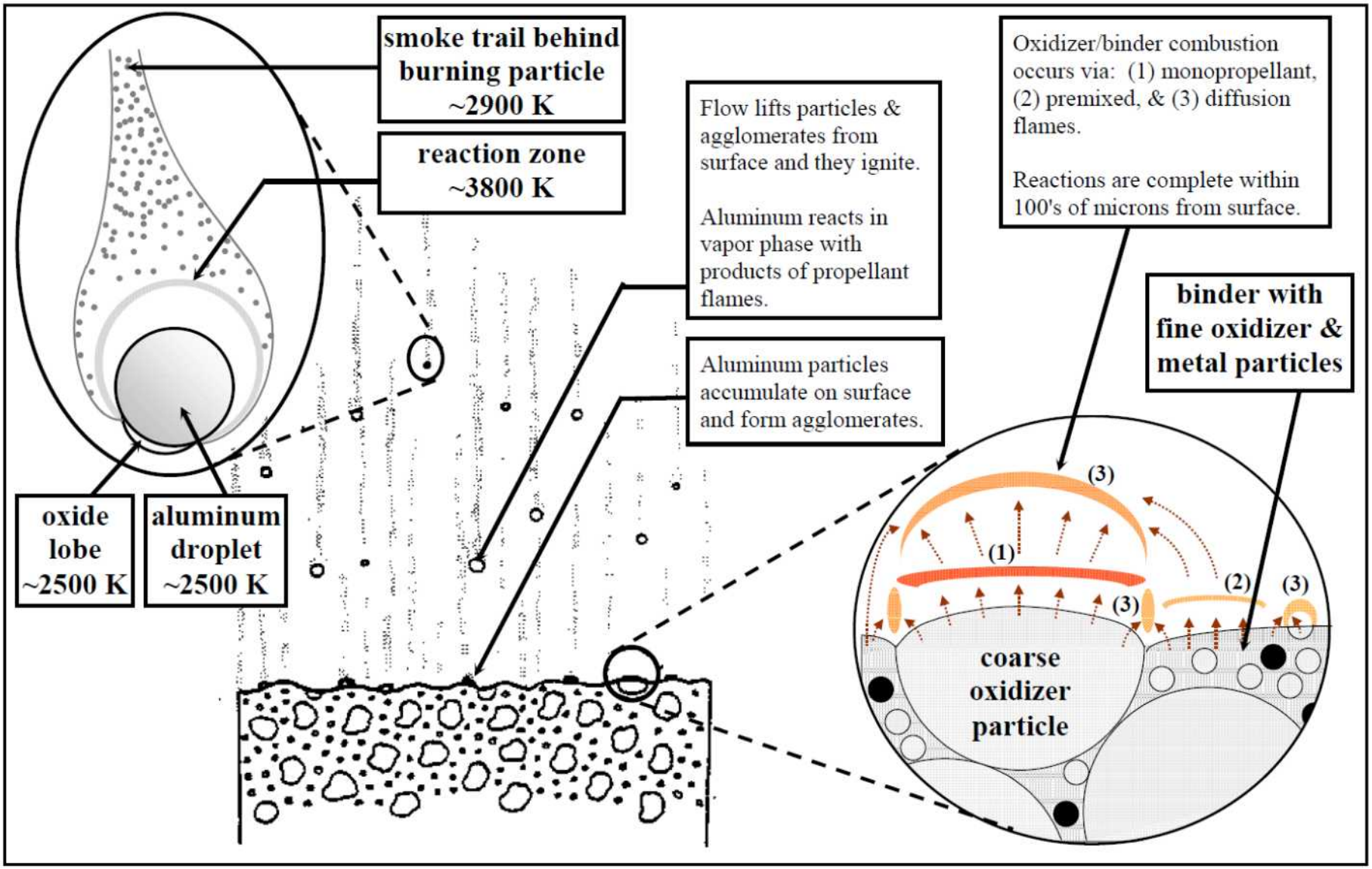

Figure from Erikson (2001).

Aluminum Droplet Formation Videos

0.24 inch

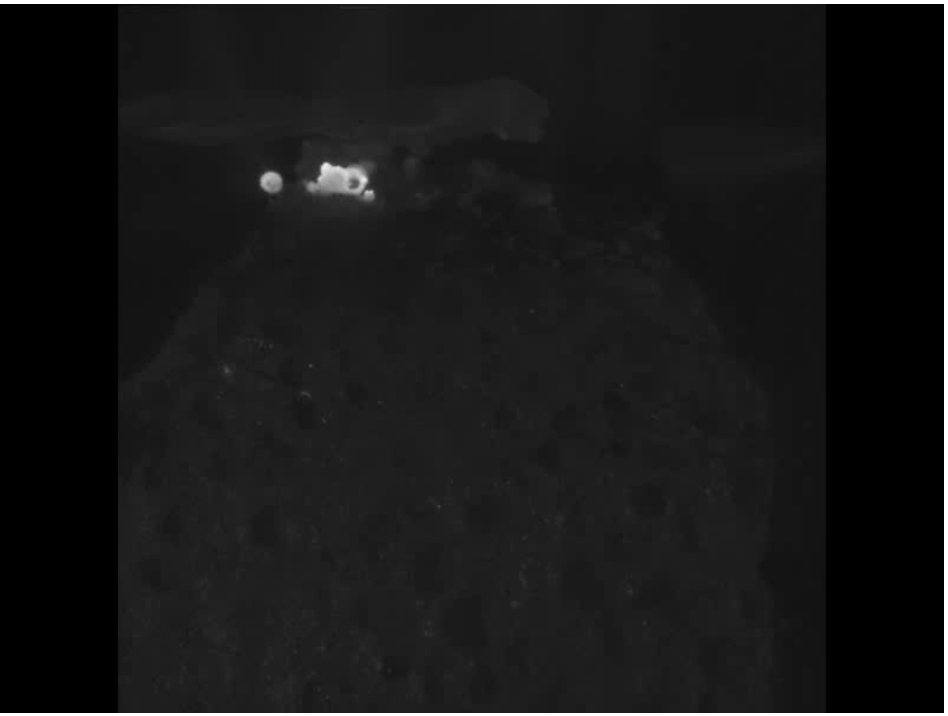

Video of Atlas (Aerojet) propellant burning at ambient pressure (Lyle and Atwood, 2006). Shutter speed 1/1000 second and 1000 frames per second.

0.24 inch

Video of a propellant burning at 100 psi in nitrogen (Ward, Atwood, and Bui, 2006).

Aluminum Droplet Combustion Model

- The model for aluminum evaporation accounts for energy transfer to the droplet, evaporation from the droplet, combustion of the evaporated aluminum, and the energy release due to combustion
- Conserved scalars are introduced to facilitate the solution
- One conserved scalar is formed from the specific enthalpy conservation equation combined with oxidizer conservation equations times the enthalpies of reaction for each oxidizer,

$$\beta_{T-O} = \int_{T_0}^{T} c_p dT + \frac{Y_O W_F q_{comb}}{\upsilon_O W_O}$$

Only one oxidizer shown, but actually there are three.

- Another conserved scalar is formed from the fuel and oxidizer species equations

$$\beta_{F-O} = \frac{Y_F}{\upsilon_F W_F} - \frac{Y_O}{\upsilon_O W_O}$$

Only one oxidizer shown, but actually there are three.

- Solutions to the conservation equations have the form

$$\xi_{k,f} = \dot{m}_0 \int_{r_p}^{\infty} \frac{dr}{4\pi r^2 (\rho D_k)} = \ln(1 + B_k)$$

$$B_k = \frac{\beta_{k,\infty} - \beta_{k,f}}{-\left.\frac{\partial \beta_k}{\partial \xi_k}\right|_f}$$

All equations from Hewson et al (2007).

Aluminum Droplet Combustion Model

- Solving for the evaporation rate using the temperature – oxidizer conserved scalar

$$\xi_{T,f} = \dot{m}_0 \int_{r_p}^{\infty} \frac{dr}{4\pi r^2 \left(\lambda / c_p\right)} = \ln[1 + B_{T-O}] \qquad \text{where} \qquad B_{T-O} = \frac{\int_{T_f}^{T_\infty} c_{p,\infty} dT + \frac{Y_{O,\infty} W_F q_{comb}}{\upsilon_O W_O}}{h_{vap} + \frac{Q_{rad}}{\dot{m}} + \left(\frac{m_p c_{v,p}}{\dot{m}} \frac{dT_p}{dt} \right)}$$

introducing $$Nu_f = \left(2 r_p c_{p,eff} \left. \frac{dT}{dr} \right|_f \right) \Bigg/ \left(\int_{T_f}^{T_\infty} c_{p,\infty} dT + \frac{Y_{O,\infty} W_F q_{comb}}{\upsilon_O W_O} \right)$$

then $$\dot{m} = \dot{m}_0 \frac{Nu_f}{Nu_{f,Re=0}} = \dot{m}_0 \left(1 + 0.3 Re^{1/2} Pr^{1/3}\right) \qquad \text{where} \qquad Pr = \frac{c_{p,f} \mu_f}{\lambda_f}$$

so $$\dot{m} = 4\pi r_p \left(\frac{\lambda}{c_p} \right)_{eff} \frac{Nu_f}{Nu_{f,Re=0}} \ln[1 + B_{T-O}] \qquad \text{where} \qquad \left(\frac{\lambda}{c_p} \right)_{eff} = \left[4\pi r_p \int_{r_p}^{\infty} \frac{dr}{4\pi r^2 \left(\lambda / c_p\right)} \right]^{-1},$$

All equations from Hewson et al (2007).

Aluminum Droplet Combustion Model

- Solving for the evaporation rate using the fuel - oxidizer conserved scalar

$$\xi_{F,f} = \dot{m}_0 \int_{r_p}^{\infty} \frac{dr}{4\pi r^2 \left(\rho D_F\right)} = \ln[1 + B_{F-O}] \qquad \text{where} \qquad B_{F-O} = \frac{Y_{F,f} - Y_{F,\infty} + \dfrac{Y_{O,\infty} W_F}{\upsilon_O W_O}}{Y_{F,p} - Y_{F,f}}$$

introducing $$Sh_f = \left(-2 r_p \left. \frac{dY_F}{dr} \right|_f \right) \Bigg/ \left(Y_{F,f} - Y_{F,\infty} + \frac{Y_{O,\infty} W_F}{\upsilon_O W_O} \right)$$

then $$\dot{m} = \dot{m}_0 \frac{Sh_f}{Sh_{f,Re=0}} = \dot{m}_0 \left(1 + 0.3 Re^{1/2} Sc^{1/3}\right)$$ where $$Sc = \frac{\mu_f}{\rho_f D_f}$$

so $$\dot{m} = 4\pi r_p \left(\rho D_F\right)_{eff} \frac{Sh_f}{Sh_{f,Re=0}} \ln[1 + B_{F-O}]$$ where $$\left(\rho D_F\right)_{eff} = \left[4\pi r_p \int_{r_p}^{\infty} \frac{dr}{4\pi r^2 \left(\rho D_F\right)} \right]^{-1}$$

All equations from Hewson et al (2007).

Aluminum Droplet Combustion Model

- Closures for remaining terms

Assume the film temperature and aluminum mass fraction are related through the Clausius-Clapeyron relationship.

$$P_{F,f} = P_{ref} \exp\left[-\frac{h_{vap}}{R}\left(\frac{1}{T_f} - \frac{1}{T_{ref}} \right) \right]$$

Use an empirical relationship to relate the heat of vaporization at the film temperature to the heat of vaporization at a reference temperature.

$$h_{vap} = h_{vap,ref} \left(\frac{T_{crit} - T_f}{T_{crit} - T_{ref}} \right)^{0.38}$$

Relate the particle heat-up to the temperature difference between the particle and the film, using a Nusselt number internal to the particle (not the same as the Nusselt number discussed previously).

$$m_p c_{v,p} \frac{dT_p}{dt} = 2\pi r_p Nu_p \lambda_p (T_f - T_p)$$

Use an empirical correlation for Nusselt number that depends upon Peclet number.

$$Nu_p = 6.58 \left\{ 1.86 + 0.86 \tanh\left[2.245 \log_{10}\left(Pe_p / 30 \right) \right] \right\}$$

Equations for Peclet number.

$$Pe_p = \frac{2\rho_p c_{v,p} U_{surface} r_p}{\lambda_p} \qquad U_{surface} = \frac{12.69 \left| \mathbf{u}_p - \mathbf{u}_g \right| Re_p^{1/3}}{16} \left(\frac{\mu_g}{\mu_p} \right)$$

All equations from Hewson et al (2007).